Molecular Biology of the Cell
Vol. 18, 1670–1682, May 2007

The RBCC Gene *RFP2* (*Leu5*) Encodes a Novel Transmembrane E3 Ubiquitin Ligase Involved in ERAD

Mikael Lerner,* Martin Corcoran,* Diana Cepeda,* Michael L. Nielsen,† Roman Zubarev,† Fredrik Pontén,‡ Mathias Uhlén,§ Sophia Hober,§ Dan Grandér,* and Olle Sangfelt*

*Department of Oncology/Pathology, Cancercentrum Karolinska, SE-171 76 Stockholm, Sweden; †Laboratory for Biological and Medical Mass Spectrometry, Uppsala Biomedical Centrum, 751 23 Uppsala, Sweden; ‡Department of Genetics and Pathology, Rudbeck Laboratory, Uppsala University, SE-751 85 Uppsala, Sweden; and §Department of Biotechnology, KTH/Alba Nova University Center, SE-106 91 Stockholm, Sweden

Submitted March 29, 2006; Revised January 29, 2007; Accepted February 6, 2007
Monitoring Editor: William Tansey

***RFP2*, a gene frequently lost in various malignancies, encodes a protein with RING finger, B-box, and coiled-coil domains that belongs to the RBCC/TRIM family of proteins. Here we demonstrate that Rfp2 is an unstable protein with auto-polyubiquitination activity in vivo and in vitro, implying that Rfp2 acts as a RING E3 ubiquitin ligase. Consequently, Rfp2 ubiquitin ligase activity is dependent on an intact RING domain, as RING deficient mutants fail to drive polyubiquitination in vitro and are stabilized in vivo. Immunopurification and tandem mass spectrometry enabled the identification of several putative Rfp2 interacting proteins localized to the endoplasmic reticulum (ER), including valosin-containing protein (VCP), a protein indispensable for ER-associated degradation (ERAD). Importantly, we also show that Rfp2 regulates the degradation of the known ER proteolytic substrate CD3-δ, but not the N-end rule substrate Ub-R-YFP (yellow fluorescent protein), establishing Rfp2 as a novel E3 ligase involved in ERAD. Finally, we show that Rfp2 contains a C-terminal transmembrane domain indispensable for its localization to the ER and that Rfp2 colocalizes with several ER-resident proteins as analyzed by high-resolution immunostaining. In summary, these data are all consistent with a function for Rfp2 as an ERAD E3 ubiquitin ligase.**

INTRODUCTION

The RBCC/TRIM (RING finger, B-box, coiled-coil/tripartite motif) group of proteins is an evolutionarily conserved family with more than 60 members. RBCC proteins are involved in diverse cellular processes, such as apoptosis (Kimura *et al.,* 2003), proliferation (Urano *et al.,* 2002), differentiation (Lalonde *et al.,* 2004), and transcriptional regulation (Wang *et al.,* 2004). One functionally uncharacterized RBCC member is the Rfp2 protein (also termed Leu5 and Trim13). The *RFP2* gene was initially cloned during the search for genes located in the commonly deleted 13q14 locus in B-CLL (B-cell chronic lymphocytic leukemia). 13q14 deletions or translocations are present in ~50% of all CLL cases (Fitchett *et al.,* 1987; Liu *et al.,* 1997; Stilgenbauer *et al.,* 2000; Mertens *et al.,* 2002). Considering all genes in the minimal deleted region, *RFP2* is the only gene with protein encoding potential and might therefore be regarded as a prime tumor suppressor gene candidate within the CLL deletion locus at 13q14 (Corcoran *et al.,* 2004). Of note is that this locus is also targeted for deletion in other hematological malignancies such as myeloma (Shaughnessy *et al.,* 2000; Elnenaei *et al.,* 2003; Schmidt-Wolf *et al.,* 2006), mantle cell lymphoma (Bigoni *et al.,* 2001), and diffuse large cell lymphoma (Wada *et al.,* 2000). Deletions have also been reported in several solid tumors such as head and neck tumors (Maestro *et al.,* 1996) and oral tumors (Ogawara *et al.,* 1998).

The *RFP2* gene was recently shown to have coding potential for two separate open reading frames (ORFs), the RBCC protein Rfp2/Leu5 and Dltet (Corcoran *et al.,* 2004), a protein with high similarity to BTB/POZ domain–containing proteins. Structurally, RBCC proteins generally contain a RING (Really Interesting New Gene) finger domain, one or two B boxes, and a coiled-coil domain (Reymond *et al.,* 2001; Torok and Etkin, 2001). RING finger domains are cysteine- and histidine-rich motifs that bind two zinc ions. They mediate protein–protein interactions (Borden, 2000) and are frequently involved in proteolysis (Pickart, 2001). B-boxes are domains with as of yet unknown function with the ability to bind one zinc ion (Borden, 1998). Like RING fingers, coiled-coil domains also mediate protein–protein interactions and have furthermore been shown to be important for homo- and heterodimerization of RBCC family members (Jensen *et al.,* 2001). Often, it seems that the entire RBCC domain is needed for proper function and intracellular localization of proteins containing these motifs, indicating that this multidomain structure acts as one functional unit (Reymond *et al.,* 2001).

A limited number of the RBCC proteins have been implicated in proteolysis, acting as E3 ubiquitin ligases by pro-

This article was published online ahead of print in *MBC in Press* (http://www.molbiolcell.org/cgi/doi/10.1091/mbc.E06–03–0248) on February 21, 2007.

Address correspondence to: Olle Sangfelt (olle.sangfelt@ki.se).

Abbreviations used: RFP2, Ret finger protein 2; Ub, ubiquitin; Ub_n, polyubiquitinated products; Ubc, ubiquitin-conjugating enzyme.

moting the attachment of the conserved polypeptide ubiquitin to specific substrates targeted for degradation (Trockenbacher *et al.*, 2001; Urano *et al.*, 2002; Vichi *et al.*, 2005). E3 ligases can be divided into two major families: HECT (Homologue of E6-AP C-terminus) domain E3s and RING finger domain E3s (Pickart, 2001). RBCC proteins with E3 ligase activity accordingly form a subset of the latter family.

One important role of the ubiquitin-proteasome system is to mediate the retrotranslocation and turnover of membrane and secretory proteins from the ER through a set of processes collectively termed ERAD (Meusser *et al.*, 2005). As a general surveillance mechanism, cells utilize the ERAD machinery to degrade proteins that are misfolded (McCracken and Brodsky, 2005; Denic *et al.*, 2006). Additionally, proteins usually part of multisubunit complexes are similarly degraded when not assembled together with their normal oligomerization partner(s). An example of the latter is the degradation of individual subunits of the T-cell receptor (Yang *et al.*, 1998). Once a protein is targeted for ERAD, E2-conjugating enzymes specific to the ER and ER-associated E3 ubiquitin ligases, such as Hrd1 and gp78, cooperate to attach ubiquitin molecules to the target (Fang *et al.*, 2001; Botero *et al.*, 2002; Kikkert *et al.*, 2004). With the help of the Cdc48/VCP-Ufd1-Npl4 complex of proteins, the ubiquitinated substrate is finally extracted from the ER membrane and degraded by the 26S proteasome (Ye *et al.*, 2001; Jarosch *et al.*, 2002). Protein degradation at the level of the ER has attracted increased attention because ERAD has been implicated in a wide variety of conformational diseases, such as Parkinson's disease and Alzheimer's disease, as well as in cancer (Takahashi and Imai, 2003; Khan *et al.*, 2004; Lindholm *et al.*, 2006; Nakamura *et al.*, 2006). Still, the molecular mechanisms underlying this process are poorly understood and a limited number of E3 ubiquitin ligases of the ER have been described.

Given the important biological function of other RBCC proteins and the frequent loss of the *RFP2* gene in CLL and other malignancies, a functional characterization of the gene is highly warranted. In the present study we present evidence that Rfp2 belongs to a previously uncharacterized subgroup of RBCC proteins containing a transmembrane domain, a domain necessary for Rfp2 to properly associate with the ER. We further demonstrate that Rfp2 can regulate the turnover of a heterologous ERAD substrate, CD3-δ, and that wild-type Rfp2 has auto-polyubiquitination activity in vitro. In conclusion, these results together define Rfp2 as a novel ER E3 ubiquitin ligase and link Rfp2 to the very limited set of proteins currently known to function as effectors of ERAD.

MATERIALS AND METHODS

Cell Lines, Transfections, and Expression Analysis

HEK293 and U2OS cells were maintained in DMEM containing 10% FBS, 2 mM glutamine, 100 U/ml penicillin, and 100 g/ml streptomycin.

For transfection experiments, HEK293 and U2OS cells were transfected with TransIT-LT1 Transfection Reagent (Mirus, Madison, WI) according to the manufacturer's protocol. RNA interference (RNAi) experiments were performed with TransIT-TKO Transfection reagent according to the manufacturer's instructions (Mirus). Small interfering RNA (siRNA) duplexes targeting either a region in exon 3 of Rfp2 or a region in exon 1 of Dltet were designed and purchased from Dharmacon (Boulder, CO; http://www.dharmacon.com/sidesign). As controls, scrambled siRNAs or siRNA duplexes against green fluorescent protein were used. siRNA sequences can be obtained from the authors upon request.

If not otherwise indicated, cells were harvested 48 h after transfection and subsequently lysed in M-RIPA buffer (150 mM NaCl, 1% Nonidet P-40, 0.5% deoxycholic acid, 0.05% SDS, 50 mM Tris, pH 7.4). Lysis buffer was supplied with Complete protease inhibitor cocktail (Roche, Indianapolis, IN), 1 mM phenylmethylsulphonylfluoride (PMSF), 1 mM sodium orthovanadate, 5 mM sodium fluoride (Sigma, St. Louis, MO). Lysates were subjected to SDS-PAGE and transferred to PVDF membranes, and the proteins were detected by Western blot analysis using an enhanced chemiluminescence system (ECL, Amersham Biosciences, Piscataway, NJ).

For immunoprecipitation experiments, cells were lysed in M-RIPA or NP-40 (150 mM NaCl, 1% Nonidet P-40, 50 mM Tris, pH 7.4) containing 10 mM *N*-ethylmaleimide (Pierce, Rockford, IL). One milligram of precleared lysate was incubated with Rfp2 antibody (500 ng) at 4°C overnight, followed by incubation with Gammabind G Sepharose beads (Amersham Biosciences) for 1 h. The beads were washed five times with lysis buffer and immunoprecipitated proteins were subjected to SDS-PAGE and Western blot analysis. For glutathione *S*-transferase (GST) pulldown, 1 mg of total protein lysate was incubated with glutathione Sepharose 4B (Amersham Biosciences) at 4°C overnight. The resin was washed five times and analyzed as described above. For GST-pulldown in denaturing conditions, cells were lysed in NP-40 buffer containing 1% SDS to disrupt noncovalent interactions. The lysate was subsequently diluted 10 times with NP-40 buffer without SDS, and pulldown was performed as described above.

For protein stability experiments, cells were treated with 30 μM MG-132 (Biomol, Plymouth Meeting, PA) for the indicated time points. For cycloheximide chase experiments, cells were treated with 100 μg/ml cycloheximide (Biomol) in the presence or absence of MG-132. Cells were harvested at the indicated time points.

Cell cycle distribution of Rfp2 expression was examined by flow cytometry analysis as described previously (Panaretakis *et al.*, 2003). DNA was stained by addition of propidium iodide staining solution (Nordic BioSite, Täby, Sweden) 20 min before flow analysis.

Constructs

The full-length coding regions of the *RFP2* and *DLTET* ORFs were separately PCR amplified with Advantage enzyme (BD Biosciences) and cloned into pEBG GST- and Tag2B FLAG-tagged vectors (Invitrogen, Carlsbad, CA). The sequence of the cloned cDNA was verified in its entire length by sequencing. The *RFP2*[$C^{13}A$] mutant was constructed using the QuikChange II XL Site-Directed Mutagenesis Kit (Stratagene, La Jolla, CA). Primers used for cloning can be obtained from the authors upon request. The *RFP2*-Δ*RING* deletion mutant was generated by cutting the *RFP2* construct with PstI and subsequently religating. The resulting ORF encodes 317 amino acids and completely lacks the RING domain. *RFP2*-Δ*TM* was constructed by PCR amplification using the reverse primer deltaTMR (ttttccatcgatgggcttgcaggcaaattagagg) together with a forward primer in frame with the ATG, resulting in the 3′-deletion of 131 amino acids, including the transmembrane domain.

Untagged pME18S-FL3-*RFP2* expression constructs were kindly provided by Dr. Akio Matsuda (Laboratory for Biology, Institute for Life Science Research, Health Care Company, ASAH1 KASEI Corporation, Shizuoka, Japan). ECFP-*VCP* plasmid was kindly provided by Dr. Florian Salomons (Department of Cellular and Molecular Biology, Karolinska Institute, Solna, Sweden). *CD3-δ*-YFP and *Ub-R*-YFP expression constructs were kindly provided by Dr. Nico Dantuma (Department of Cellular and Molecular Biology, Karolinska Institute, Solna, Sweden).

Antibodies

The following primary antibodies were used: rabbit polyclonal against Rfp2 (see below), mouse monoclonal against GST (B-14, Santa Cruz Biotechnology, Santa Cruz, CA), rabbit polyclonal against GST (Z5, Santa Cruz Biotechnology), mouse monoclonal against FLAG (M2, Stratagene), rabbit polyclonal against hemaglutinin (HA) (Y11, Santa Cruz Biotechnology), mouse monoclonal against β-tubulin (Sigma), mouse monoclonal against β-actin (Sigma), rabbit polyclonal against GAPDH (Abcam, Cambridge, MA), mouse monoclonal against Bcl-2 (124, DAKO, Carpinteria, CA), mouse monoclonal against c-Myc (9E10, Santa Cruz Biotechnology), mouse monoclonal against green fluorescent protein (GFP; Roche), rabbit polyclonal against GFP (Sigma), and horseradish peroxidase (HRP)-conjugated goat antibody against biotin (Cell Signaling). As secondary antibodies HRP-conjugated anti-rabbit and anti-mouse antibodies (Cell Signaling, Beverly, MA) were used.

To generate a novel mono-specific antibody recognizing Rfp2, a protein fragment from the coiled-coil region of Rfp2 (amino acids 158–300) was chosen because of the low sequence similarity to all other human proteins. Subsequently, primers were designed and used in RT-PCR, resulting in a gene encoding the protein fragment (Agaton *et al.*, 2003). Production, purification, and characterization of the protein fragment were performed as previously described (Agaton *et al.*, 2003). Antibody purification was performed by a depletion chromatography step, where antibodies directed toward the His-ABP-part of the fusion protein were removed and a second purification allowed for capture of the specific antibodies (Agaton *et al.*, 2004). Characterization of the antibodies was done according to a previous study (Nilsson *et al.*, 2005).

Subcellular Fractionation

Cytosolic, membranous, and nuclear extracts were prepared using the Qproteome Cell Compartment Kit according to the manufacturer's protocol (Qia-

gen, Chatsworth, CA). Briefly, sequential addition of different buffers to cell pellets followed by incubation and centrifugation results in the isolation of different cellular compartments. First buffer selectively disrupts the plasma membrane without solubilizing it, resulting in the isolation of cytosolic proteins. Plasma membranes and compartmentalized organelles remain intact and are pelleted by centrifugation. The pellet from the first step is resuspended in the second buffer, which solubilizes the plasma membrane as well as all organelle membranes except the nuclear membrane. This fraction contains membrane proteins (including proteins from the ER membrane) and proteins from the lumen of organelles (e.g., the ER and mitochondria). In the final step nuclei are solubilized using the third buffer in which all soluble and most membrane-bound nuclear proteins are extracted. Compartment separation was analyzed by immunodetection of stated marker proteins.

Metabolic Labeling

HEK293 cells were transfected with *CD3-δ*-YFP or *Ub-R*-YFP together with indicated constructs or siRNAs. After 24 h, transfectants were incubated for 30 min in methionine-/cysteine-free medium and then metabolically pulsed with 70 μCi ^{35}S cell-labeling mix (Redivue ProMix ^{35}S, Amersham Biosciences) at 37°C for 30 min. After the pulse, cells were washed, chased in complete medium supplemented with 10 mM methionine and 1 mM cysteine (Sigma), and harvested at the indicated time points in M-RIPA lysis buffer. CD3-δ-YFP and Ub-R-YFP were immunoprecipitated using rabbit polyclonal GFP antibody (Sigma) and the level of metabolically labeled YFP construct was subsequently analyzed by SDS-PAGE and autoradiography.

Isolation of Protein Complexes for Mass Spectrometry

To prepare protein extracts for subsequent mass spectrometric analysis, ~5×10^7 HEK293 cells were used. Because Rfp2 was shown to be a strictly membrane-associated protein, soluble cytosolic proteins were discarded in order to reduce complexity of the sample. Washed cell pellets were resuspended in hypotonic lysis buffer (10 mM NaCl, 3 mM $MgCl_2$, 20 mM Tris, pH 7.5), incubated for 10 min with shaking, and centrifuged at 3600 rpm for 10 min. Supernatants containing soluble cytosolic proteins were discarded, and cell pellets were lysed in NP-40 buffer. Endogenous Rfp2 protein was immunoprecipitated as described above using 2 μg of Rfp2 antibody and proteins were subjected to SDS-PAGE with subsequent staining with SimplyBlue Safestain (Invitrogen). In parallel, other control proteins were similarly immunoprecipitated and analyzed. Samples were run in different gels or some distance apart to minimize cross-contamination. Entire lanes were cut into 10-kDa pieces, and proteins were identified by nanoflow liquid chromatography tandem mass spectrometry as described below. Only peptides exclusively present in Rfp2 immunoprecipitated samples were regarded as possible Rfp2 interacting proteins.

Nanoflow Liquid Chromatography Tandem Mass Spectrometry

All experiments were performed on a 7-tesla LTQ-FT mass spectrometer (Thermo Electron, Bremen, Germany), modified with a nanoelectrospray ion source (Proxeon Biosystems, Odense, Denmark). The high-performance liquid chromatography setup used in conjunction with the mass spectrometer (LC-MS) consisted of a solvent degasser, nanoflow pump, and thermostated microautosampler (Agilent 1100 nanoflow system, Wilmington, DE). Chromatographic separation of peptides was achieved on a 15-cm fused silica emitter (75-μm inner diameter, Proxeon Biosystems) packed in-house with a methanol slurry of reverse-phased, fully end-capped Reprosil-Pur C18-AQ 3 μm resin (Dr. Maisch GmbH, Ammerbuch-Entrigen). Briefly, the tryptic peptides were autosampled onto the packed column at a flow rate of 500 nL/min and then eluted at a flow rate of 200 nl/min using a linear gradient of 4.5–40.5% acetonitrile in 0.5% acetic acid over 90 min and ionized by an applied voltage of 1.8 kV to the emitter.

Analysis was performed using unattended data-dependent acquisition mode, in which the mass spectrometer automatically switches between a high-resolution survey scan (resolution = 100,000 at m/z 400), followed by acquisition of both an electron capture dissociation (ECD; Zubarev *et al.*, 2000) and collision activated dissociation (CAD) tandem mass spectra (resolution = 25,000) of the two most abundant peptides eluting at this moment from the nano-LC column. Complementary fragmentation of the same peptide yielded different fragment ions that increased the specificity of the sequence information. Using this complementary information (Horn *et al.*, 2000) for protein ID not only improves the confidence in protein identification performed by search engines, but for a fixed confidence level also identifies a larger number of peptides and proteins than when only one fragmentation technique is used (Nielsen *et al.*, 2005).

All data from the acquired MS/MS spectra was extracted into so-called dta-files using TurboSequest software (Thermo), and an in-house written Java program was used for extraction of complementary fragment masses before database searching, as described previously (Nielsen *et al.*, 2005; Savitski *et al.*, 2005). The new dta-files containing complementary fragment masses was merged into a single file, which was searched using the Mascot Search Engine (Matrix Science, Boston, MA; Perkins *et al.*, 1999) against the full IPI human database (version 3.15; downloaded February 2006) with carbamidomethyl cysteine as fixed modification and oxidized methionine and ubiquitination on lysine as variable modifications. Peptide searches were performed with an initial tolerance on mass measurement of 3 ppm in MS mode and 0.02 Da in MS/MS mode. Only proteins uniquely identified by a minimum of two significant peptides were taken into consideration for this study.

In Vitro Ubiquitination Assays

HEK293 cells were transfected with GST-tagged *pEBG*, *DLTET*, *RFP2*, or *RFP2*[$C^{13}A$] expression plasmids. Forty-eight hours after transfection, cells were harvested in LSLD buffer (50 mM NaCl, 0.1% Tween-20, 10% glycerol, 50 mM HEPES) with protease inhibitor cocktail. Two milligrams of total protein was used for GST pulldown as described above. Precipitates were extensively washed (five times each in LSLD buffer and 20 mM Tris, pH 7.5), and in vitro reactions were performed directly on the beads. The in vitro reactions contained 20 ng human recombinant E1, 200 ng E2, 2 μg biotinylated ubiquitin (BioMol), 5 mM ATP, 5 mM MgCl2, 1 mM DTT, 1 U inorganic pyrophosphatase, 10 mM creatine phosphate, 2.5 U creatine phosphokinase from rabbit muscle (Sigma) in 20 mM Tris, pH 7.5, to a final volume of 50 μl. As E2s, UbcH5b and [C^{85}A]UbcH5b were used. [C^{85}A]UbcH5b is a catalytically inactive mutant incapable of forming thiol ester conjugates. The reactions were incubated at 37°C for 60–120 min and stopped by boiling in 1× NuPAGE LDS Sample Buffer (Invitrogen). Ubiquitinated proteins were detected by Western blot analysis using biotin antibodies.

Immunofluorescence Analysis

U2OS cells and HEK293 were transfected as described. Cells on coverslips were fixed in 4% formaldehyde for 10 min, permeabilized with 0.2% Triton X-100 in PBS for 10 min, and blocked with blocking buffer (2% BSA, 0.2% Tween-20, 5% glycerol in PBS) for 30 min at room temperature. They were incubated with primary antibodies (anti-Rfp2 diluted 1:100, anti-Myc diluted 1:50) for 1 h at room temperature followed by appropriate secondary antibodies conjugated with fluorescein isothiocyanate (FITC; 1:40; DAKO), Texas Red (1:200; Vector Laboratories, Burlingame, CA) or Alexa Fluor 594 (1:500; Molecular Probes, Eugene, OR). Slides were mounted using Vectashield with DAPI (Vector Laboratories), and images were acquired on a Zeiss Axioplan 2 imaging microscope with Axiovision software (Thornwood, NY) and processed either as gray scale or dual color TIFF images in Adobe Photoshop (Adobe Systems, San Jose, CA). Mock-transfected cells were used as negative controls.

RESULTS

Rfp2 Is an Unstable Protein Regulated by the Proteasomal System

As a first step in characterizing the Rfp2 protein, epitope-tagged constructs of *RFP2* were expressed in HEK293 cells by transient transfection. HEK293 cells were also transfected with expression constructs encoding Dltet, the second ORF present within the *RFP2* gene locus (Corcoran *et al.*, 2004). The expression of transfected GST-tagged Dltet was robust, and the detected amount was roughly equal to that of the GST tag alone. In contrast, the amount of GST-tagged Rfp2 protein was significantly lower (>10 times lower as assessed by quantification of band intensity; Figure 1A). The same phenomenon with low amount of Rfp2 protein was observed with other expression vectors, and in another cell type (HeLa cells, data not shown). One reason for the reduced amount of Rfp2 protein in cells could be that only a small subset of cells expresses Rfp2. However, this possibility was ruled out because flow cytometric DNA histogram analysis in HEK293 cells together with staining for endogenous Rfp2 expression using a specific Rfp2 antibody (see below) revealed that the protein is similarly expressed in all cells, regardless of cell cycle phase (data not shown). To address whether the low levels of Rfp2 protein could be due to high turnover of the protein, we next examined whether Rfp2 levels are increased in cells treated with proteasomal inhibitors. As can be seen in Figure 1B, treatment with the proteasomal inhibitor MG-132 markedly increased Rfp2 protein levels. Together these data show that Rfp2 is an inherently unstable protein regulated by the proteasomal system. In the following experiments, we focused our analysis on characterizing the Rfp2 protein.

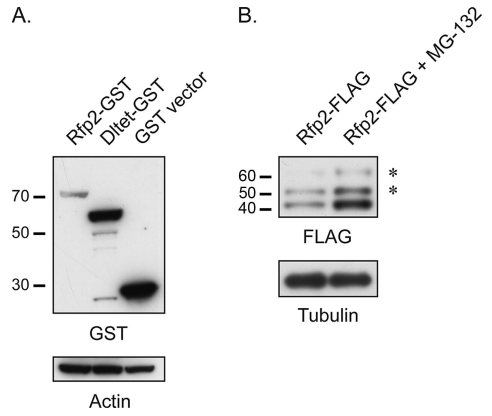

Figure 1. Rfp2 is an unstable protein that becomes stabilized with proteasomal inhibition. (A) HEK293 cells were transfected with GST-tagged Rfp2, Dltet, and empty vector, and exogenous protein expression was detected with monoclonal antibodies against GST. (B) Steady state levels of transfected FLAG-tagged Rfp2 in HEK293 cells after treatment with 30 μM MG-132 for 4 h. Rfp2 protein was detected with FLAG antibodies. Asterisks indicate Rfp2 conjugated with single ubiquitin molecules (see below). Actin and tubulin were used as loading controls as indicated. Numbers indicate protein size in kDa.

A polyclonal antibody directed against the coiled-coil domain of Rfp2 (amino acids 158–300) was generated. The predicted size of endogenous Rfp2 protein is ~47 kDa, and a band of approximately that size was observed in untransfected HEK293 lysates after long exposure, suggesting that the Rfp2 antibody recognizes the low levels of endogenous Rfp2 protein (data not shown). We next silenced Rfp2 expression in HEK293 cells with siRNA oligos specific for Rfp2. As can be seen in Figure 2A, significant reduction of ectopically expressed FLAG-tagged Rfp2 was only observed in cells transfected with Rfp2-specific siRNA oligos, whereas control oligos had no effect on Rfp2 protein levels. Finally, we knocked down endogenous Rfp2 protein in HEK293 cells, confirming the predicted size of Rfp2 and demonstrating the prominent affinity of the antibody for the Rfp2 protein (Figure 2B).

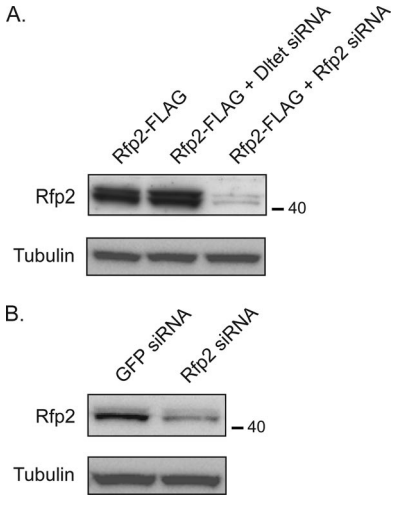

Figure 2. Specificity of a novel polyclonal Rfp2 antibody. (A) To monitor the specificity of the Rfp2 antibody, plasmids expressing FLAG-tagged Rfp2 were cotransfected with siRNA oligos targeting *RFP2* and *DLTET*, respectively. Blots were developed using Rfp2-specific polyclonal antibodies to detect exogenous Rfp2 protein. (B) Extracts of HEK293 cells treated with *RFP2* siRNA oligos, and siRNA oligos targeting green fluorescent protein (GFP) were analyzed for endogenous Rfp2 expression by Western blotting with Rfp2 antibody. Numbers indicate protein size in kDa. Detection of tubulin was used as loading control.

Rfp2 Is Ubiquitinated in Cells

Interestingly, MG-132 treatment or long exposure of filters probed with Rfp2 antibodies revealed the existence of additional distinct bands, of higher molecular weight, extending upward from the Rfp2 band (Figure 1B). In most cells, endogenous Rfp2 protein was detected as two major bands, but in some cases up to three bands were visible (Figures 1B and 3A). This, together with the fact that the Rfp2 protein is regulated by the proteasomal system, prompted us to investigate whether these additional bands represent ubiquitinated conjugates of Rfp2. To this end, we ectopically expressed GST-Rfp2 in parallel with an empty GST-vector in HEK293 cells. Lysates were prepared and Rfp2 protein was immunoprecipitated with Rfp2 antibodies, separated on SDS-PAGE gels and subsequently stained with Coomassie (Figure 3B). Bands of expected and higher molecular weight were observed exclusively in the lane containing transfected Rfp2 protein (indicated by arrowheads). Distinct bands were excised and analyzed by nanoflow liquid chromatography tandem mass spectrometry (LC-MS/MS) as previously described (Shevchenko *et al.*, 2000; Nielsen *et al.*, 2005). Although the band corresponding to the predicted size of GST-tagged full-length Rfp2 (73 kDa, band 1) only contained tryptic peptides from Rfp2 and GST, both the slower migrating bands (bands 2 and 3) were additionally found to contain peptides of ubiquitin (see table in Figure 3B). These results suggest that Rfp2 is covalently conjugated with single ubiquitin molecules (mono- and/or oligoubiquitination). From these mass spectrometric analyses, however, we were unable to detect any diagnostic branched ubiquitin peptides between Rfp2 and the C-terminus of ubiquitin and could therefore not determine the exact Rfp2 lysine residue(s) conjugated to ubiquitin.

To directly demonstrate the occurrence of mono-ubiquitinated Rfp2 species, cells were cotransfected with GST-tagged Rfp2 and an HA-tagged ubiquitin expression plasmid. Pulldowns of Rfp2 were separated in high-resolution gels and immunoblotted in parallel with antibodies for tagged ubiquitin and Rfp2. As can be seen in Figure 3C, the Rfp2 antibody detected two bands of approximately 8-kDa difference in size. Conversely, the HA-antibody only showed immunoreactivity for the upper, slower migrating band, identifying this band as Rfp2 conjugated to a single ubiquitin molecule.

RING-dependent Auto-Polyubiquitination of Rfp2 In Vivo

A common feature of E3 ubiquitin ligases is their ability to auto-polyubiquitinate and degrade themselves, possibly as a precautionary mechanism to limit their levels in the lack of specific substrates (Nuber *et al.*, 1998; Canning *et al.*, 2004). Because such an activity is an indication of E3 ligase function; we investigated whether Rfp2 is polyubiquitinated in cells. To detect only Rfp2 conjugated with ubiquitin, cells were transfected with GST-tagged Rfp2 together with HA-ubiquitin and lysed under denaturing conditions to disrupt noncovalent interactions. Samples were diluted with lysis buffer, and GST-Rfp2 was precipitated with glutathione beads and resolved on SDS-PAGE, and blots were subsequently hybridized with HA antibodies. As can be seen in Figure 4A, high-molecular-weight smears representing polyu-

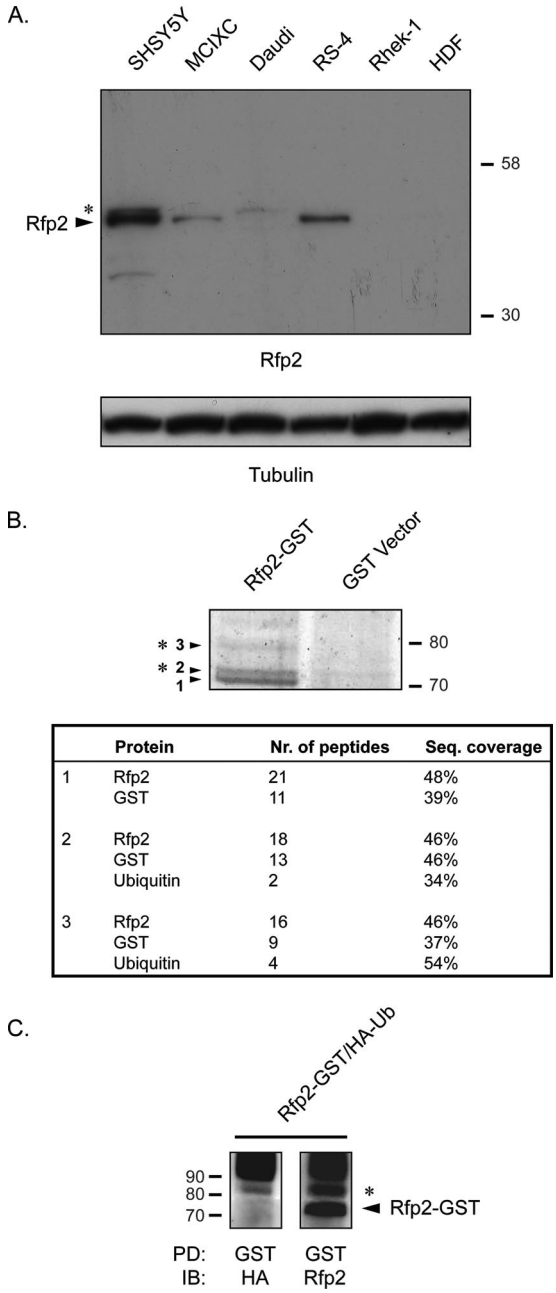

	Protein	Nr. of peptides	Seq. coverage
1	Rfp2	21	48%
	GST	11	39%
2	Rfp2	18	46%
	GST	13	46%
	Ubiquitin	2	34%
3	Rfp2	16	46%
	GST	9	37%
	Ubiquitin	4	54%

Figure 3. Rfp2 is monoubiquitinated in cells. (A) Analysis of endogenous protein levels of Rfp2 in a panel of human cell lines. Protein lysates were prepared from neuroblastoma (SHSY5Y), neuroepithelioma (SK-N-MCIXC), Burkitt's lymphoma (Daudi), acute lymphoblastic leukemia (RS-4), keratinocyte (Rhek-1), and human diploid fibroblast (HDF) cells and subjected to Western blot analysis with Rfp2 antibodies. Nonubiquitinated Rfp2 is marked with a solid arrowhead, and asterisks indicate Rfp2 conjugated with single ubiquitin molecules. Tubulin was used as a loading control. (B) Identification of Rfp2 bands with higher molecular weight as ubiquitinated forms of the protein. GST-tagged Rfp2 and an empty vector were expressed in HEK293 cells, precipitated with Rfp2 antibodies, separated by SDS-PAGE, and visualized with Coomassie. Each Rfp2 band was excised, subjected to in-gel tryptic digestion, and analyzed by mass spectrometry. The bands analyzed are marked with numbers (1–3) and solid arrowheads. High-molecular-mass Rfp2 bands are marked with asterisks (monoubiquitinated Rfp2). Boxed text summarizes the mass spectrometric data and indicates the number of peptides identified and corresponding sequence coverage of the isolated nonubiquitinated (band 1) and monoubiquitinated Rfp2 protein bands (bands 2 and 3). (C) GST-Rfp2 was overexpressed together with HA-tagged ubiquitin in HEK293 cells and precipitated with glutathione beads. This was followed by Western blot analysis with HA antibodies to detect ubiquitinated Rfp2 (left) and Rfp2 antibodies to detect both unconjugated and ubiquitinated Rfp2 (panel). Molecular size markers are shown on either side in kDa.

biquitinated Rfp2 were observed under these conditions (Figure 4A, left).

To determine whether the RING domain of Rfp2 is essential for auto-polyubiquitination activity in vivo, we generated a deletion mutant, Rfp2-ΔRING, lacking this domain. Cells were cotransfected with HA-ubiquitin together with untagged full-length Rfp2 or Rfp2-ΔRING. Rfp2 was immunoprecipitated with Rfp2 antibodies, and HA antibodies were used to detect ubiquitinated Rfp2. As can be seen in Figure 4B, full-length Rfp2 was heavily polyubiquitinated, in contrast to the Rfp2-ΔRING mutant that virtually lacked the high-molecular-weight smear (Figure 4B, top panel). These results strongly suggest that the RING domain is required for auto-polyubiquitination activity of Rfp2. In line with the polyubiquitination deficiency of Rfp2-ΔRING, total protein levels of this mutant accumulated several magnitudes above the levels of wild-type Rfp2 protein (Figure 4B, bottom panel). Similar stabilization was observed when a single conserved cysteine in the Rfp2 RING domain was mutated to alanine (Rfp2[$C^{13}A$]; Figure 4C, left). Additionally, cycloheximide chase experiments demonstrated that the Rfp2[$C^{13}A$] mutant was stable throughout the incubation period, in contrast to wild-type Rfp2, which was rapidly degraded (Figure 4C, right).

Interestingly, even though the Rfp2-ΔRING mutant (as well as the Rfp2[$C^{13}A$] point mutant) is deficient in polyubiquitination, it can still be modified with single ubiquitin molecules (Figure 4B, bottom panel, and data not shown). Together, these results indicate that although modification of Rfp2 with single ubiquitin molecules occurs in a RING-independent manner, polyubiquitination and subsequent degradation of Rfp2 requires an intact RING domain.

Rfp2 E3 Ubiquitin Ligase Activity Catalyzes Auto-Polyubiquitination In Vitro

Rfp2 E3 ubiquitin ligase activity was further examined by a series of in vitro reactions. GST-tagged Rfp2 was incubated in vitro at 37°C together with recombinant human E1, the E2 enzyme UbcH5b, biotinylated ubiquitin, and ATP. As can be seen in Figure 5A, clear accumulation of polyubiquitinated Rfp2 products was observed. In reactions where wild-type UbcH5b was substituted with a mutated, catalytically inactive variant, UbcH5b[$C^{85}A$], this auto-polyubiquitination was abolished. Moreover, when GST-Rfp2 was replaced with GST-Dltet or GST alone, polyubiquitination did not occur (Figure 5A). Additionally, no polyubiquitination was observed when ATP was omitted, demonstrating the specific ATP-dependent nature of the reaction (data not shown).

To rule out the possibility that in vitro polyubiquitination of Rfp2 is due to E2-only mediated modification of a misfolded Rfp2 protein, we also performed in vitro reactions with the Rfp2[$C^{13}A$] mutant, lacking one conserved cysteine essential for RING-mediated polyubiquitination. As opposed to wild-type Rfp2, both the RING deletion and the point mutant were found to be deficient in generating polyubiquitinated Rfp2 species (Figure 5B and data not shown), Together, these experiments demonstrate that Rfp2 has E3

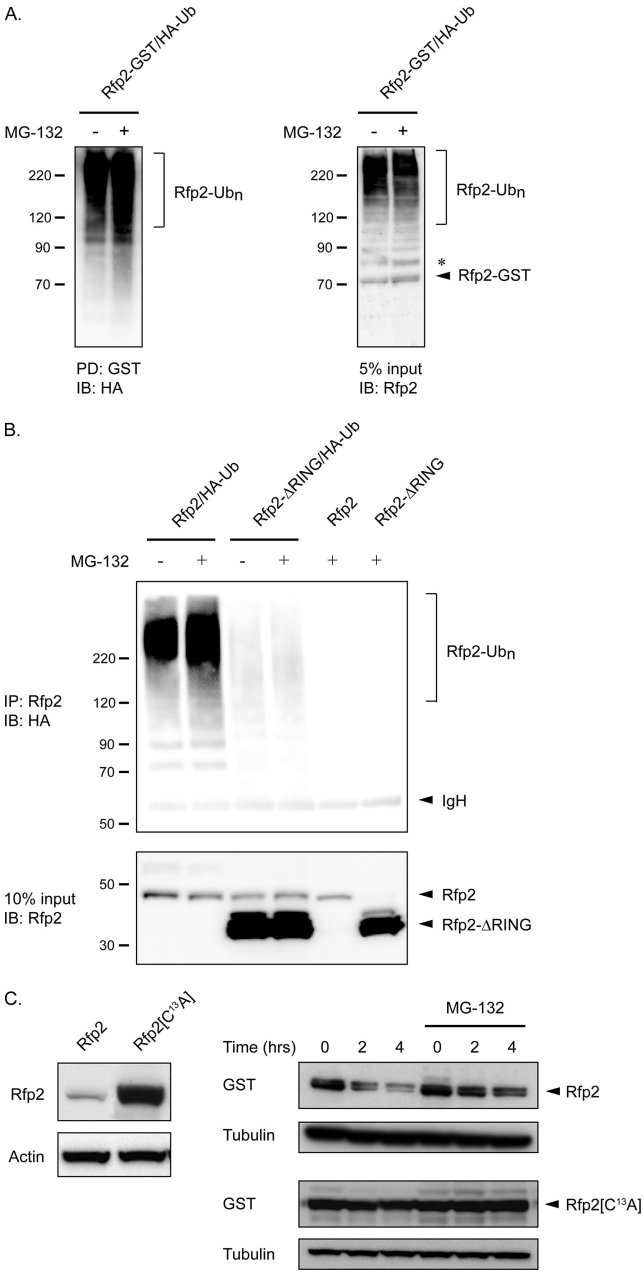

Figure 4. Rfp2 is polyubiquitinated in cells in a RING-dependent manner. (A) Polyubiquitination of Rfp2. Left panel, cotransfection of GST-Rfp2 and HA-ubiquitin into HEK293 cells was followed by cell lysis under denaturing conditions to disrupt noncovalent interactions. Rfp2 was precipitated using glutathione beads, and Western blot analysis with HA antibodies was used to detect high-molecular-weight smears indicative of ubiquitinated Rfp2 conjugates. In cells treated with MG-132 (30 μM) ubiquitinated Rfp2 conjugates accumulate. Right panel, Western blot of whole cell lysate using 5% of the input used for glutathione precipitation. Rfp2 antibodies detect both unubiquitinated and polyubiquitinated forms of Rfp2. Nonubiquitinated Rfp2 is marked with a solid arrowhead, and asterisks indicate Rfp2 conjugated with single ubiquitin molecules. Numbers indicate protein size in kDa. (B) RING-dependent polyubiquitination of Rfp2. Top panel, HEK293 cells were transfected with indicated constructs and immunoprecipitated with Rfp2 antibodies. Where indicated MG-132 (30 μM) was added for 4 h before harvesting. Ubiquitinated proteins were visualized with HA antibodies. Polyubiqutinated smears (marked with brackets) are seen in samples transfected with full-length Rfp2 but not with the RING deletion mutant Rfp2-ΔRING. Solid arrowhead indicates immunoglobulin heavy chain from the immunoprecipitation. Bottom panel, Western blot of whole cell lysate using 10% of the input used for immunoprecipitation showing stabilization of the Rfp2-ΔRING mutant. Rfp2 and Rfp2-ΔRING are marked with solid arrowheads. Numbers indicate protein size in kDa. (C) Stabilization of the Rfp2[C^{13}A] mutant. Left panel, Western blot analysis of HEK293 cells ectopically expressing wild-type Rfp2 or Rfp2[C^{13}A] with Rfp2 antibodies showing stabilization of the mutant protein. Actin was used as a loading control. Right panel, steady state levels of transfected GST-tagged Rfp2 and Rfp2[C^{13}A] in HEK293 cells at various indicated time points after cycloheximide treatment in the presence or absence of MG-132. Western blot with GST antibodies shows stabilization of the Rfp2 point mutant irrespective of proteasomal inhibition. Tubulin was used as a loading control.

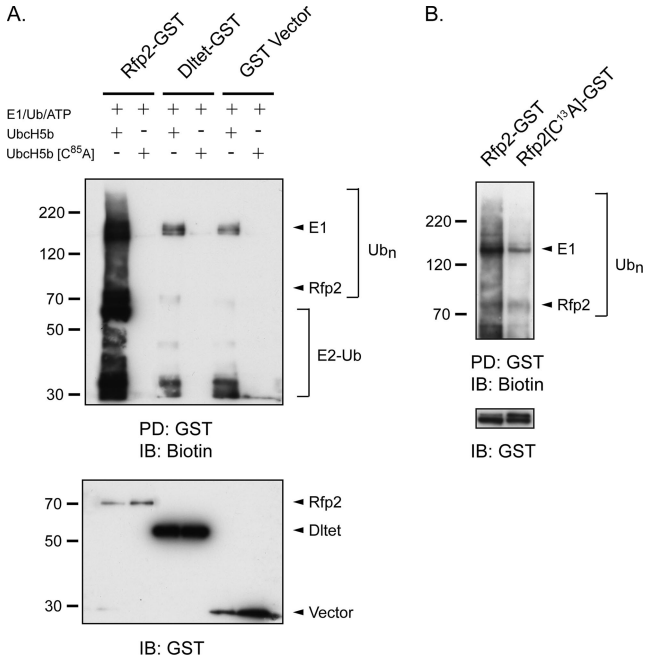

Figure 5. RING-dependent E3 ligase activity of Rfp2 in vitro. (A) In vitro ubiquitination assay with UbcH5b or UbcH5b [C^{85}A], together with GST-tagged Rfp2, Dltet or empty vector, respectively. GST-tagged proteins, expressed in HEK293 cells, were precipitated with glutathione beads, extensively washed, and incubated together with E1, the E2 enzyme UbcH5b, biotinylated ubiquitin, and ATP (top panel). Polyubiquitination, as detected by Western blot with biotin antibodies, is exclusively observed in the presence of catalytically active UbcH5b, and Rfp2 (top panel). Polyubiquitinated proteins are marked with a bracket. The indicated band appearing at about 135 kDa represents ubiquitinated E1. Bands below Rfp2 (indicated with a solid arrowhead) represent proteolytic fragments of Rfp2 as well as ubiquitinated E2 conjugates. (B) In vitro reaction with wild-type Rfp2 and Rfp2[C^{13}A] showing extensive polyubiquitination with Rfp2, but not with Rfp2[C^{13}A] (top panel). Lower panels, Western blot with GST antibodies showing amount of GST-tagged product in each lane. Numbers indicate protein size in kDa.

ubiquitin ligase activity in vitro, and we conclude that the *RFP2* gene encodes an RBCC E3 ubiquitin ligase.

Rfp2 Is Part of a Novel RBCC-Transmembrane Subgroup

Bioinformatic analysis of the RBCC family reveals that although the N-terminal domains are very similar between different RBCC family members, the C-terminal domains are diverse and include SPRY, NHL, BROMO, and FN3 domains (Figure 6A; Jensen *et al.*, 2001; Reymond *et al.*, 2001;

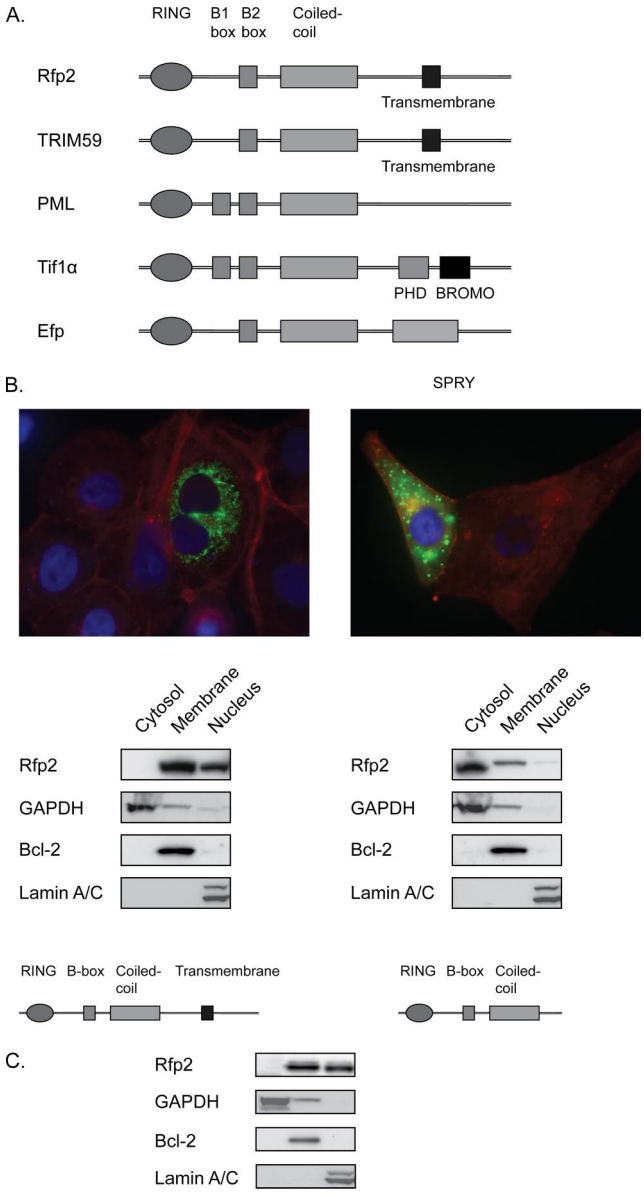

Figure 6. Rfp2 is a membrane-bound protein. (A) Schematic representation of selected RBCC proteins showing the varied C-terminal ends. (B) Top, U2OS cells were transfected with wild-type Rfp2 and with Rfp2-ΔTM, respectively. Forty-eight hours after transfection, cells were fixed in 4% formaldehyde, permeabilized with 0.2% Triton X-100 in PBS, and stained with Rfp2 antibodies. Primary antibodies were visualized with FITC-conjugated anti-rabbit IgG, and F-actin fibers were visualized with Texas Red–conjugated phalloidin. DAPI was used to stain the nucleus. Bottom panel, HEK293 cell lysates transfected with Rfp2 and Rfp2-ΔTM were fractionated as described in *Material and Methods,* and fractions were analyzed by Western blotting for Rfp2 and a set of indicated marker proteins. Wild-type Rfp2 is localized to the membranous and nuclear fraction, whereas Rfp2-ΔTM is relocalized to the cytosol. Schematic figures represent the Rfp2 variants used in the transfections. (C) Subcellular fractionation of HEK293 followed by Western blotting for endogenous Rfp2 protein confirms the subcellular localization observed with ectopically expressed protein.

Meyer *et al.*, 2003; Balint *et al.*, 2004). Interestingly, bioinformatic analysis of the structure of Rfp2 showed that it lacks these commonly described C-terminal domains, but instead contains a single C-terminal transmembrane domain (present at amino acid positions 319–341) as predicted by TMHMM analysis (http://www.cbs.dtu.dk/services/TMHMM). This particular domain structure (RING, B-box, coiled-coil, transmembrane) has not yet been described in any other RBCC protein, and detailed analysis of all RBCCs (70 in total) shows that this structure is also found in one additional family member, namely TRIM59, the protein most homologous to Rfp2 (Figure 6A). Notably, this particular domain structure was not mentioned in a recent study that subclassified RBCCs according to C-terminal domain composition (Short and Cox, 2006). The functionally uncharacterized TRIM59 gene is located at chromosome 3q25, within a >1 Mb region paralogous to 13q14 (Chang *et al.*, 2002). The Rfp2 and TRIM59 proteins are evolutionary conserved to the level of Fugu and can thus be considered to form a novel RBCC-transmembrane subgroup.

Rfp2 Is a Membrane-bound Protein Localized to the ER

To examine in detail where Rfp2 is expressed in cells and if it colocalizes with any particular membranous structures, deletion constructs were generated and ectopically expressed in HEK293 and U2OS cells. Although full-length Rfp2 protein localized to the perinuclear area of the cell in a reticular, speckled manner (Figure 6B, top left), a mutant lacking the C-terminal portion including the transmembrane domain, Rfp2-ΔTM, was expressed throughout the cytoplasm (Figure 6B, top right). The localization of Rfp2 was further studied by fractionation of HEK293 cell lysates into cytosolic, membranous, and nuclear compartments. Full-length Rfp2 was strictly present in the membranous and nuclear fractions (Figure 6B, bottom left), in contrast to the Rfp2-ΔTM mutant that was relocalized to the soluble cytosolic fraction (Figure 6B, bottom right), a finding in accordance with the immunofluorescence stainings. Collection of multiple focal planes (*z*-stacks) obtained from immunofluorescence microscopy clearly demonstrated that the Rfp2 protein is restricted to the nuclear membrane and is absent from the interior of the nucleus (Figure 6B and data not shown). The same membrane-associated pattern was observed when analyzing endogenous Rfp2 protein by fractionation (Figure 6C). These experiments show that Rfp2 is localized to cytoplasmic and nuclear membranes and that this membrane association is dependent on the C-terminus of Rfp2 containing the transmembrane domain.

The speckled cytoplasmic staining observed for Rfp2 has previously not been characterized. In a recent study of more than 30 RBCCs by Reymond *et al.* (2001), colocalization studies failed to identify any specific organelles associated with this expression pattern. On the basis of our fractionation results and the fact that the Rfp2 staining pattern is reminiscent of ER localization, we ectopically expressed Rfp2 together with the ER-localized mammalian E2-conjugating enzyme mmUbc6 and stained for both these proteins in U2OS cells. As can be seen in Figure 7A, top panel, Ubc6 was found to colocalize with Rfp2. Specificity of staining was ascertained by using Rfp2 antibodies as well as two different tag antibodies (GST and FLAG) to detect Rfp2 (data not shown). Finally, immunofluorescence analysis of endogenous Rfp2 protein in HEK293 confirmed that it is distributed in a similar manner as ectopically expressed Rfp2 protein in U2OS cells (Figure 7, bottom panel).

Together these results define Rfp2 as a membrane-associated protein that localizes to the ER.

Rfp2 Regulates the Stability of the ERAD Substrate CD3-δ

Because Rfp2 localizes to the ER and has ubiquitin ligase activity, we decided to determine whether Rfp2 is involved

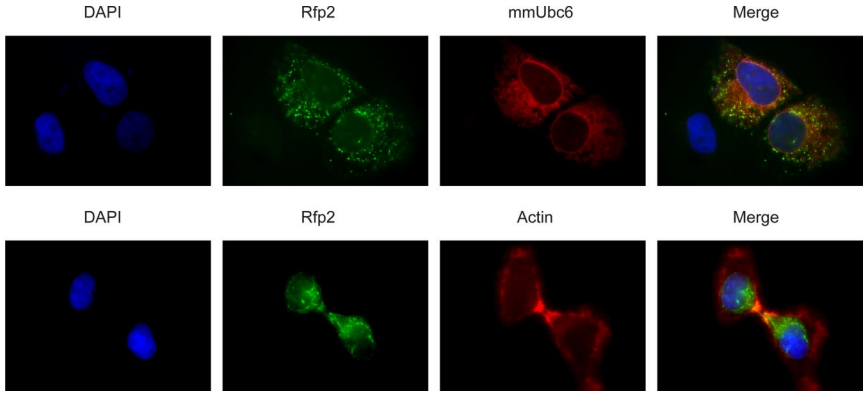

Figure 7. Rfp2 colocalizes with the ER. Top panel, U2OS cells were cotransfected with Rfp2 and Myc-mmUbc6, processed as described in *Material and Methods,* and costained with Rfp2 and Myc antibodies. Rfp2 is visualized with FITC-conjugated anti-rabbit IgG, whereas mmUbc6 is visualized with Texas Red–conjugated anti-mouse IgG. DAPI was used to stain nuclei. Merged pictures (far right) show considerable overlap between Rfp2 and mmUbc6 staining. Bottom panel, immunofluorescence staining for endogenous Rfp2 in HEK293 cells using Rfp2 antibodies. Texas Red–conjugated phalloidin visualizes F-actin fibers.

in ERAD by testing whether it can mediate the turnover of a known ERAD substrate. The CD3-δ subunit of the T-cell receptor complex is one such well-established substrate when expressed in the absence of the other receptor subunits (Klausner *et al.,* 1990). HEK293 cells were transiently transfected with CD3-δ-YFP together with wild-type Rfp2 and the Rfp2[$C^{13}A$] mutant, respectively. Next, cycloheximide chase experiments were performed to examine the turnover of CD3-δ in vivo. As expected, CD3-δ was rapidly degraded in control cells transfected with an empty vector. In contrast, cotransfection of the Rfp2[$C^{13}A$] mutant significantly stabilized CD3-δ protein (Figure 8A). These results suggest that the Rfp2[$C^{13}A$] mutant exerts a dominant negative effect, preventing the degradation of CD3-δ. Ectopic expression of wild-type Rfp2 had a slight effect on the total levels of CD3-δ, as evident from reduced levels at time point zero, but the rate of degradation did not seem to be significantly altered. In accordance with a putative role for Rfp2 in CD3-δ degradation, high-resolution immunostaining showed clear colocalization of Rfp2 and CD3-δ in U2OS cells ectopically expressing these proteins (Figure 8B).

Inhibition of protein synthesis by cycloheximide will lead to substantial degradation of Rfp2 itself during the chase period. To circumvent the problem with possible depletion of the Rfp2 pool in the presence of cycloheximide, pulse-chase experiments using metabolically labeled proteins were also performed. As can be seen in Figure 9A, expression of the Rfp2[$C^{13}A$] mutant stabilized CD3-δ compared with an empty vector control, a finding in line with the cycloheximide experiments. Again, overexpression of wild-type Rfp2 did not appear to have any significant effect on CD3-δ turnover (data not shown). In experiments where CD3-δ was replaced by the N-end rule substrate Ub-R-YFP (Dantuma *et al.,* 2000), significant stabilization of the substrate could not be observed in the presence of the Rfp2[$C^{13}A$] mutant (Figure 9B).

To examine the role of endogenous Rfp2 in CD3-δ turnover, Rfp2 expression was knocked down using siRNA. To avoid possible off-target effects, two different siRNAs targeting Rfp2 were used. Pulse-chase analysis showed that silencing of Rfp2, using either oligo, led to significant stabilization of CD3-δ compared with cells transfected with a scrambled siRNA oligo (Figure 9C). In summary, these experiments demonstrate that Rfp2 functions as a RING-dependent ERAD E3 ubiquitin ligase and regulates the degradation of the ER substrate, CD3-δ.

Rfp2 Associates with the AAA-ATPase VCP

In an attempt to further define the function of Rfp2 in cells, a mass spectrometric approach was undertaken to identify

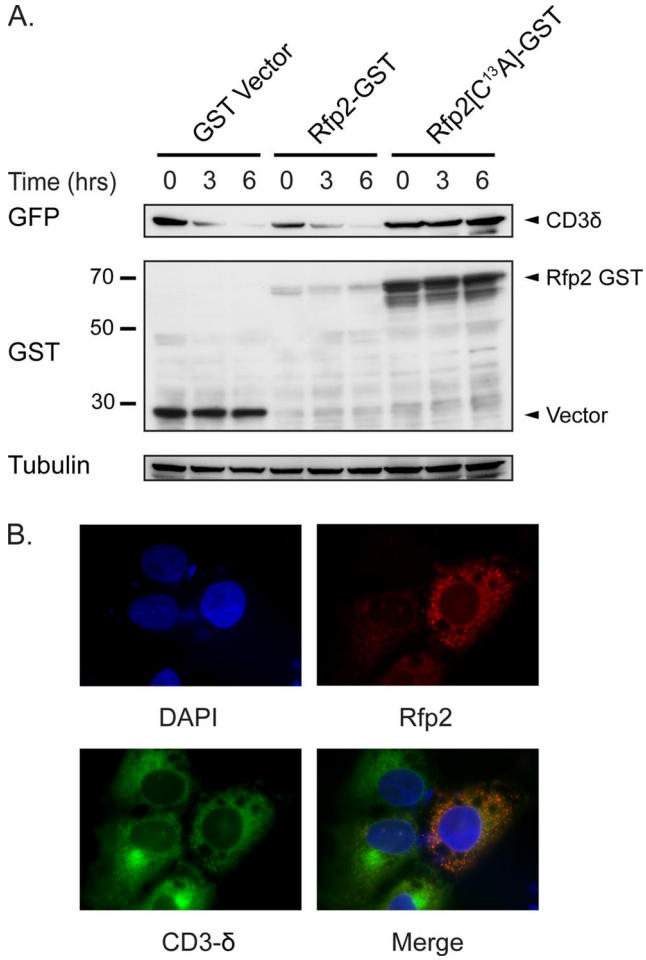

Figure 8. Rfp2[$C^{13}A$] stabilizes the ERAD substrate CD3-δ. (A) Cycloheximide chase analysis of CD3-δ turnover. HEK293 cells were transfected with CD3-δ-YFP together with the indicated GST constructs. Twenty-four hours after transfection cells were subjected to cycloheximide treatment and harvested at indicated time points. CD3-δ abundance was monitored by Western blot analysis using GFP antibodies (top panel). The GFP antibody recognizes the YFP tag fused to CD3-δ. Cells expressing Rfp2[$C^{13}A$] exhibit marked stabilization of CD3-δ, compared with control cells. Middle panel, Western blot with GST antibodies showing amount of GST-tagged product in each lane. Tubulin was used as a loading control (bottom panel). (B) Colocalization of Rfp2 and CD3-δ. U2OS cells were cotransfected with Rfp2 and CD3-δ-YFP, processed as described in *Material and Methods,* and stained with Rfp2 antibodies. Rfp2 is visualized with Alexa Fluor 594–conjugated anti-rabbit IgG. DAPI was used to stain nuclei. Merged pictures (far right) show considerable overlap between Rfp2 staining and CD3-δ-YFP.

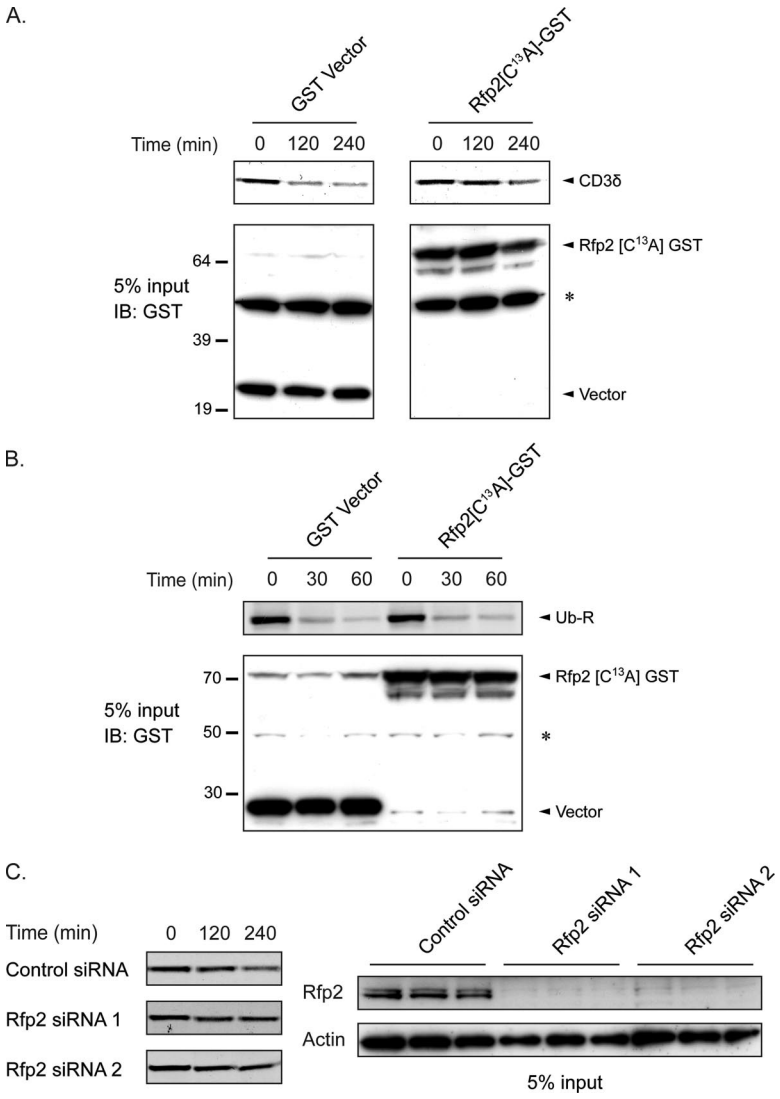

Figure 9. Rfp2 degrades the ERAD substrate CD3-δ. (A) Metabolic pulse-chase analysis of CD3-δ turnover showing stabilization of CD3-δ in the presence of Rfp2[$C^{13}A$]. HEK293 cells transfected with indicated constructs were labeled with [^{35}S] cell labeling mix and chased in complete medium for the indicated times. CD3-δ turnover was monitored by autoradiography (top panel). (B) Rfp2[$C^{13}A$] does not affect Ub-R-YFP stability. Autoradiography after metabolic pulse-chase analysis of Ub-R shows no stabilization of substrate in the presence of Rfp2[$C^{13}A$] (top panel). Bottom panels, Western blot of whole cell lysate using 5% of the input used for immunoprecipitation showing amount of GST-tagged product in each lane. Numbers indicate protein size in kDa. Asterisk indicates an unspecific band. (C) Knockdown of Rfp2 expression stabilizes CD3-δ. HEK293 cells were transfected with CD3-δ-YFP together with two different Rfp2 siRNA oligos or scrambled control oligos, respectively, and CD3-δ turnover was analyzed by metabolic labeling (left panels). Right panel, Western blot on 5% input controls showing effective silencing of Rfp2.

putative interacting partners for Rfp2. Lysates were prepared from untransfected HEK293 cells and Rfp2-associated protein complexes were immunoprecipitated with Rfp2 antibodies, separated on SDS-PAGE gels, and stained with Coomassie (Figure 10A). Entire lanes were cut into smaller pieces and LC-MS/MS was used to obtain sequence information of putative Rfp2-interacting proteins. In parallel, immunoprecipitates obtained with a set of irrelevant antibodies were also analyzed as controls. Peptides unique for Rfp2 immunoprecipitates were regarded as putative Rfp2-interacting proteins (Figure 10A).

In line with the results described above, Rfp2 immunoprecipitates were found to contain a significant number of peptides from several proteins residing in the ER, including VCP, sarcoplasmic/endoplasmic reticulum calcium ATPase 2 (SERCA2A), dolichol-diphosphooligosaccharide-protein glycosyltransferase (DDOST), and calmodulin (see table in Figure 10A).

VCP, a protein directly linked to ERAD was identified with a very high accuracy due to the detection of a peptide unique for this protein (MDELQLFR with oxidized methionine; data not shown). To confirm the interaction between Rfp2 and VCP, human ECFP-tagged VCP was cotransfected with different GST-tagged Rfp2 constructs in HEK293 cells. GST pulldowns were resolved on SDS-PAGE gels and probed with GFP antibodies (recognizing the ECFP tag). As can be seen in Figure 10B, VCP copurified with wild-type Rfp2 but not with Rfp2 mutants lacking the transmembrane and coiled-coil domains. From this experiment, it appears that the C-terminal part of Rfp2 including the transmembrane domain is necessary for its interaction with VCP. To rule out the possibility of spurious interactions due to overexpression artifacts, the interaction between endogenous Rfp2 and VCP was also tested. ECFP-VCP was transfected alone, endogenous Rfp2 was immunoprecipitated, and the blot was probed with GFP antibodies. The appearance of a distinct VCP band after Western blot analysis showed that VCP protein interacts with endogenous Rfp2, a finding in line with the mass spectrometric analysis, where endogenous VCP coimmunoprecipitated with endogenous Rfp2 (Figure 10C). In summary, these results demonstrate that the Rfp2 protein interacts with the ER-resident protein VCP, an ATPase indispensable for ERAD.

DISCUSSION

Members of the RBCC family of proteins have been shown to be involved in a number of critical intracellular processes

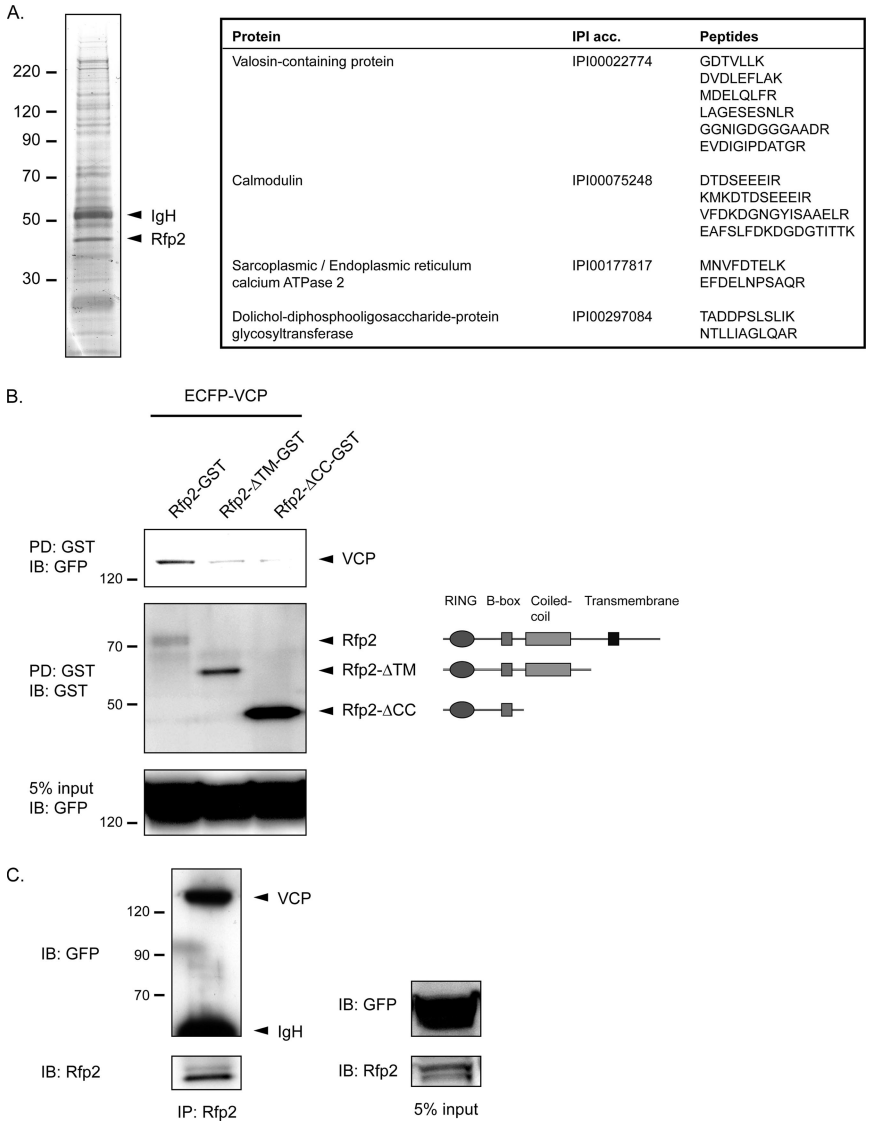

Figure 10. Rfp2 coimmunoprecipates with several ER-resident proteins. (A) MS analysis of Rfp2 protein complexes. Rfp2 immunoprecipitations were performed as described in *Material and Methods*, separated on SDS-PAGE gels, and stained with Coomassie. In parallel, a set of immunoprecipitations using irrelevant antibodies were used as controls. Entire lanes were cut into 10-kDa pieces and were analyzed by LC-MS/MS. Peptides unique for Rfp2 immunoprecipitates were regarded as putative Rfp2 interacting proteins. Boxed text lists sequences of peptides from ER-resident proteins exclusively found in Rfp2 immunoprecipitates. IPI accession numbers for the corresponding proteins are included. Numbers indicate protein size in kDa. (B) Rfp2 interacts with VCP. HEK293 were transfected with ECFP-VCP together with indicated GST constructs. Lysates were prepared in NP40 buffer and incubated with glutathione Sepharose beads. After extensive washing, proteins bound to the resin were extracted and subjected to Western blot analysis with antibodies against the indicated proteins. The GFP antibody recognizes the ECFP tag fused to VCP. A VCP band can be observed in the lane containing transfected wild-type Rfp2 protein but not in lanes containing indicated Rfp2 deletion mutants (top panel). Middle panel, Western blot with GST antibodies showing amount of GST-tagged product in each lane. Schematic figures represent the Rfp2 variants used in the transfections. Lower panel, Western blot of whole cell lysate using 5% of the input used for glutathione precipitation showing equal amounts of transfected ECFP-VCP. (C) VCP interacts with endogenous Rfp2 protein. ECFP-VCP overexpressing cells were subjected to immunoprecipitaion with Rfp2 antibodies, and VCP was detected with Western blotting using GFP antibodies. Extracts (5% of input) were immunoblotted with GFP and Rfp2 antibodies to confirm expression of VCP and Rfp2, respectively.

including differentiation, apoptosis, and tumorigenesis. In many instances both the specific enzymatic function and the intracellular localization of the protein was found to be crucial for appropriate biological function. In this study we show that Rfp2, a member of the RBCC/TRIM family of RING finger proteins, is a novel ERAD E3 ubiquitin ligase.

To date, only a few mammalian ER-associated E3 ubiquitin ligases, most containing RING and transmembrane domains, have been identified including MARCH-VI, Hrd1, and gp78/AMFR (Fang *et al.,* 2001; Kikkert *et al.,* 2004; Hassink *et al.,* 2005; Kreft *et al.,* 2006). Rfp2 is thus added to the limited, but growing, number of RBCC E3s (Trockenbacher *et al.,* 2001; Urano *et al.,* 2002; Horn *et al.,* 2004; Kallijarvi *et al.,* 2005; Vichi *et al.,* 2005). Until now, none of the characterized RBCCs have been described as ER-resident proteins. The finding that Rfp2 is an E3 ligase localized to this compartment is substantiated by a series of observations. First, Rfp2 is demonstrated to be a membrane-bound protein (Figures 6, B and C). Second, it colocalizes with several ER-resident proteins, including Ubc6 and the T-cell receptor subunit CD3-δ. Both of these features are dependent on the C-terminal part of the protein harboring a single putative transmembrane domain (Figures 6B, 7, and 8B). Third, Rfp2 has the ability to mediate the degradation of a well-known ERAD substrate, CD3-δ (Figures 8A and 9, A and C). Finally, Rfp2 is found to coimmunoprecipitate with a number of ER-resident proteins, including VCP, a protein with a central role in ERAD (Figures 10, A–C).

Central to the function of the characterized E3 ligases of the ER is their involvement in the unfolded protein response (UPR) and ERAD (Menendez-Benito *et al.,* 2005; Meusser *et al.,* 2005). Previously, these proteins were mainly implicated in general surveillance processes. However, recent evidence shows that the ERAD pathway is also required for the regulated degradation of specific ER substrates, such as the elimination of HMG-CoA reductase by gp78 (Song *et al.,* 2005). It is evident from our results that Rfp2, in common with gp78 and Hrd1, has the ability to target CD3-δ for degradation (Fang *et al.,* 2001; Kikkert *et al.,* 2004). In contrast to many of the other known ERAD substrates, such as TCRα and CFTR, CD3-δ is a protein of native conformation that is degraded in the ER when it lacks its oligomerization partners (Klausner *et al.,* 1990). It is well established that single substrates can be degraded by several different E3s (Brooks and Gu, 2006), and it is noteworthy that CD3-δ can be degraded by Rfp2, as well as by both gp78 and Hrd1. This

points to a considerable overlap in substrate specificity at the ER. One explanation for this could be that a certain amount of redundancy is required for the cell to cope with substrate overload during times of ER stress. Whether Rfp2 shares other ERAD substrates, such as TCRα or apolipoprotein B100, with gp78 and Hrd1 remains to be determined. Also, elucidation of which substrates that might be specific for Rfp2 will be instrumental in further mapping its biological function.

Two E2 conjugating enzymes have been specifically coupled to the ER, namely the mammalian homologues of yeast Ubc6p and Ubc7p. One fundamental difference between them is that although mmUbc7 (official gene name *Ube2g2*) needs to be recruited to the ER membrane by a docking protein (Biederer *et al.*, 1997; Fang *et al.*, 2001), mmUbc6 (official gene name *Ube2j2*) is permanently anchored to the ER membrane by way of its C-terminus (Lenk *et al.*, 2002). Interestingly, we have recently found that endogenous Rfp2 binds ectopically expressed mmUbc6 but not mmUbc7 (data not shown). Whether mmUbc6 represents the bona fide E2 of Rfp2 remains to be formally proven, but these data would support preferential usage of mmUbc6 over mmUbc7 by Rfp2.

The role for Rfp2 in ERAD was further supported by the identification of several ER-resident proteins in an MS screen for Rfp2-interacting proteins (Figure 10A). One of the proteins identified in the screen was VCP, and this interaction was also confirmed by in vivo coimmunoprecipitation of VCP with Rfp2 (Figure 10, B and C). VCP is a multifunctional type II AAA-ATPase that has been intimately linked to proteasomal degradation in general and ERAD in particular (Ye, 2006). VCP, in complex with Ufd1 and Npl4, is required to extract ubiquitinated proteins to the cytosol from the ER for proteolysis during ERAD (Ye *et al.*, 2001). For example, gp78 cannot mediate degradation of CD3-δ without interaction with VCP (Zhong *et al.*, 2004). One possibility is that interaction with VCP dictates substrate specificity for Rfp2. In a recent investigation, a VCP-containing complex was shown to be essential for the function of a yeast homologue to MARCH-VI, in its function to degrade membrane bound, but not soluble substrates in the ER (Ravid *et al.*, 2006).

VCP has been reported to bind to ubiquitinated proteins during the process of degradation. Therefore, one might argue that it binds Rfp2 simply because Rfp2 is a short-lived proteasomal substrate. However, the binding of VCP to Rfp2 does not seem to be correlated with the ubiquitination of Rfp2 as the Rfp2-ΔRING mutant, which is deficient in polyubiquitination, was shown to bind VCP as well (data not shown). Furthermore, binding of VCP to Rfp2 does not seem require overexpression of either protein, as immunoprecipitation of endogenous Rfp2 also yielded several VCP peptides in the MS analysis (see table in Figure 10A). From the limited interaction mapping done, it seems that the C-terminal part anchoring Rfp2 to the ER membrane is essential for VCP binding. More detailed mapping is however required to establish how these proteins interact and function together in vivo.

The *RFP2* gene has been implicated in the pathogenesis of CLL, multiple myeloma and other malignancies, due to its chromosomal location at 13q14.3, a region frequently deleted in these tumors (Kapanadze *et al.*, 1998; Elnenaei *et al.*, 2003). Preliminary studies have indicated that overexpression of the dominant negative mutant Rfp2[$C^{13}A$] increases cell proliferation in HCT116 and HEK293 cells (data not shown). These results are in line with a putative tumor suppressor function of Rfp2 although further experiments are needed to substantiate these findings and to delineate the underlying mechanism.

Recent evidence shows that altered protein degradation through defective ubiquitin-mediated proteolysis underlie many malignant diseases (Pagano and Benmaamar, 2003). Proteasome inhibitors have consequently been considered attractive candidates for cancer therapy because of their ability to induce cell cycle arrest and apoptosis (Ludwig *et al.*, 2005). In relation to the present study, both CLL and multiple myeloma cells have been demonstrated to be sensitive to proteasomal inhibition with the drug bortezomib (PS341 or Velcade; Kelley *et al.*, 2004; Mitsiades *et al.*, 2005). The fact that multiple myeloma cells have a high load of misfolded ER proteins as a consequence of the production of large amounts of immunoglobulins has been suggested to be one of the reasons why these cells are highly sensitive to proteasomal inhibitors (Obeng *et al.*, 2006). Furthermore, the UPR has been demonstrated to be essential for differentiation of B-cells, underscoring that UPR and ERAD have important roles in physiological processes (Wu and Kaufman, 2006). For example, B-cells lacking *XBP-1*, a critical signaling intermediate in UPR and the induction of ER stress, are unable to differentiate into plasma cells (Reimold *et al.*, 2001). The finding that a common genetic aberration in CLL and multiple myeloma results in deletion of an ERAD E3 ubiquitin ligase, namely *RFP2*, is in this respect intriguing. One speculative possibility is that loss of Rfp2 leads to defects in induction of the UPR and consequently impaired B-cell differentiation. How Rfp2 might be involved in UPR signaling awaits investigation, and identification of target substrates for Rfp2 ubiquitin ligase activity will be crucial to dissect the mechanism behind the putative tumor suppressor function of Rfp2 in CLL and other malignancies.

ACKNOWLEDGMENTS

The authors acknowledge the technical support provided by A. C. Björklund. This work was supported by grants from the Swedish Cancer Society, the Swedish Cancer Foundation, Gustav V Jubileumsfond, The Swedish Research Council, Karolinska Institute Foundations, the Knut and Alice Wallenberg Foundation, and the Leukaemia Research Fund. This work was partly funded by a grant from Pfizer.

REFERENCES

Agaton, C., Falk, R., Hoiden Guthenberg, I., Gostring, L., Uhlen, M., and Hober, S. (2004). Selective enrichment of monospecific polyclonal antibodies for antibody-based proteomics efforts. J. Chromatogr. A *1043*, 33–40.

Agaton, C. *et al.* (2003). Affinity proteomics for systematic protein profiling of chromosome 21 gene products in human tissues. Mol. Cell Proteomics *2*, 405–414.

Balint, I., Muller, A., Nagy, A., and Kovacs, G. (2004). Cloning and characterisation of the RBCC728/TRIM36 zinc-binding protein from the tumor suppressor gene region at chromosome 5q22.3. Gene *332*, 45–50.

Biederer, T., Volkwein, C., and Sommer, T. (1997). Role of Cue1p in ubiquitination and degradation at the ER surface. Science *278*, 1806–1809.

Bigoni, R., Cuneo, A., Milani, R., Roberti, M. G., Bardi, A., Rigolin, G. M., Cavazzini, F., Agostini, P., and Castoldi, G. (2001). Secondary chromosome changes in mantle cell lymphoma: cytogenetic and fluorescence in situ hybridization studies. Leuk. Lymphoma *40*, 581–590.

Borden, K. L. (1998). RING fingers and B-boxes: zinc-binding protein-protein interaction domains. Biochem. Cell Biol. *76*, 351–358.

Borden, K. L. (2000). RING domains: master builders of molecular scaffolds? J. Mol. Biol. *295*, 1103–1112.

Botero, D., Gereben, B., Goncalves, C., De Jesus, L. A., Harney, J. W., and Bianco, A. C. (2002). Ubc6p and ubc7p are required for normal and substrate-induced endoplasmic reticulum-associated degradation of the human selenoprotein type 2 iodothyronine monodeiodinase. Mol. Endocrinol. *16*, 1999–2007.

Brooks, C. L., and Gu, W. (2006). p53 ubiquitination: Mdm2 and beyond. Mol. Cell *21*, 307–315.

Canning, M., Boutell, C., Parkinson, J., and Everett, R. D. (2004). A RING finger ubiquitin ligase is protected from autocatalyzed ubiquitination and degradation by binding to ubiquitin-specific protease USP7. J. Biol. Chem. *279*, 38160–38168.

Chang, R., Xu, X., and Li, M. D. (2002). Molecular cloning, mapping and characterization of a novel mouse RING finger gene, Mrf1. Gene *291*, 241–249.

Corcoran, M. M. *et al.* (2004). DLEU2 encodes an antisense RNA for the putative bicistronic RFP2/LEU5 gene in humans and mouse. Genes Chromosomes Cancer *40*, 285–297.

Dantuma, N. P., Lindsten, K., Glas, R., Jellne, M., and Masucci, M. G. (2000). Short-lived green fluorescent proteins for quantifying ubiquitin/proteasome-dependent proteolysis in living cells. Nat. Biotechnol. *18*, 538–543.

Denic, V., Quan, E. M., and Weissman, J. S. (2006). A luminal surveillance complex that selects misfolded glycoproteins for ER-associated degradation. Cell *126*, 349–359.

Elnenaei, M. O., Hamoudi, R. A., Swansbury, J., Gruszka-Westwood, A. M., Brito-Babapulle, V., Matutes, E., and Catovsky, D. (2003). Delineation of the minimal region of loss at 13q14 in multiple myeloma. Genes Chromosomes Cancer *36*, 99–106.

Fang, S., Ferrone, M., Yang, C., Jensen, J. P., Tiwari, S., and Weissman, A. M. (2001). The tumor autocrine motility factor receptor, gp78, is a ubiquitin protein ligase implicated in degradation from the endoplasmic reticulum. Proc. Natl. Acad. Sci. USA *98*, 14422–14427.

Fitchett, M., Griffiths, M. J., Oscier, D. G., Johnson, S., and Seabright, M. (1987). Chromosome abnormalities involving band 13q14 in hematologic malignancies. Cancer Genet. Cytogenet. *24*, 143–150.

Hassink, G. *et al.* (2005). TEB4 is a C4HC3 RING finger-containing ubiquitin ligase of the endoplasmic reticulum. Biochem. J. *388*, 647–655.

Horn, D. M., Zubarev, R. A., and McLafferty, F. W. (2000). Automated de novo sequencing of proteins by tandem high-resolution mass spectrometry. Proc. Natl. Acad. Sci. USA *97*, 10313–10317.

Horn, E. J. *et al.* (2004). RING protein Trim32 associated with skin carcinogenesis has anti-apoptotic and E3-ubiquitin ligase properties. Carcinogenesis *25*, 157–167.

Jarosch, E., Taxis, C., Volkwein, C., Bordallo, J., Finley, D., Wolf, D. H., and Sommer, T. (2002). Protein dislocation from the ER requires polyubiquitination and the AAA-ATPase Cdc48. Nat. Cell Biol. *4*, 134–139.

Jensen, K., Shiels, C., and Freemont, P. S. (2001). PML protein isoforms and the RBCC/TRIM motif. Oncogene *20*, 7223–7233.

Kallijarvi, J., Lahtinen, U., Hamalainen, R., Lipsanen-Nyman, M., Palvimo, J. J., and Lehesjoki, A. E. (2005). TRIM37 defective in mulibrey nanism is a novel RING finger ubiquitin E3 ligase. Exp. Cell Res. *308*, 146–155.

Kapanadze, B. *et al.* (1998). A. cosmid and cDNA fine physical map of a human chromosome 13q14 region frequently lost in B-cell chronic lymphocytic leukemia and identification of a new putative tumor suppressor gene, Leu5. FEBS Lett. *426*, 266–270.

Kelley, T. W., Alkan, S., Srkalovic, G., and Hsi, E. D. (2004). Treatment of human chronic lymphocytic leukemia cells with the proteasome inhibitor bortezomib promotes apoptosis. Leuk. Res. *28*, 845–850.

Khan, M. M., Nomura, T., Chiba, T., Tanaka, K., Yoshida, H., Mori, K., and Ishii, S. (2004). The fusion oncoprotein PML-RARalpha induces endoplasmic reticulum (ER)-associated degradation of N-CoR and ER stress. J. Biol. Chem. *279*, 11814–11824.

Kikkert, M., Doolman, R., Dai, M., Avner, R., Hassink, G., van Voorden, S., Thanedar, S., Roitelman, J., Chau, V., and Wiertz, E. (2004). Human HRD1 is an E3 ubiquitin ligase involved in degradation of proteins from the endoplasmic reticulum. J. Biol. Chem. *279*, 3525–3534.

Kimura, F. *et al.* (2003). Cloning and characterization of a novel RING-B-box-coiled-coil protein with apoptotic function. J. Biol. Chem. *278*, 25046–25054.

Klausner, R .D., Lippincott-Schwartz, J., and Bonifacino, J. S. (1990). The T cell antigen receptor: insights into organelle biology. Annu. Rev. Cell Biol. *6*, 403–431.

Kreft, S. G., Wang, L., and Hochstrasser, M. (2006). Membrane topology of the yeast endoplasmic reticulum-localized ubiquitin ligase Doa10 and comparison with its human ortholog TEB4 (MARCH-VI). J. Biol. Chem. *281*, 4646–4653.

Lalonde, J. P. *et al.* (2004). HLS5, a novel RBCC (ring finger, B box, coiled-coil) family member isolated from a hemopoietic lineage switch, is a candidate tumor suppressor. J. Biol. Chem. *279*, 8181–8189.

Lenk, U., Yu, H., Walter, J., Gelman, M. S., Hartmann, E., Kopito, R. R., and Sommer, T. (2002). A role for mammalian Ubc6 homologues in ER-associated protein degradation. J. Cell Sci. *115*, 3007–3014.

Lindholm, D., Wootz, H., and Korhonen, L. (2006). ER stress and neurodegenerative diseases. Cell Death Differ. *13*, 385–392.

Liu, Y. *et al.* (1997). Cloning of two candidate tumor suppressor genes within a 10 kb region on chromosome 13q14, frequently deleted in chronic lymphocytic leukemia. Oncogene *15*, 2463–2473.

Ludwig, H., Khayat, D., Giaccone, G., and Facon, T. (2005). Proteasome inhibition and its clinical prospects in the treatment of hematologic and solid malignancies. Cancer *104*, 1794–1807.

Maestro, R., Piccinin, S., Doglioni, C., Gasparotto, D., Vukosavljevic, T., Sulfaro, S., Barzan, L., and Boiocchi, M. (1996). Chromosome 13q deletion mapping in head and neck squamous cell carcinomas: identification of two distinct regions of preferential loss. Cancer Res. *56*, 1146–1150.

McCracken, A. A., and Brodsky, J. L. (2005). Recognition and delivery of ERAD substrates to the proteasome and alternative paths for cell survival. Curr. Top. Microbiol. Immunol. *300*, 17–40.

Menendez-Benito, V., Verhoef, L. G., Masucci, M. G., and Dantuma, N. P. (2005). Endoplasmic reticulum stress compromises the ubiquitin-proteasome system. Hum. Mol. Genet. *14*, 2787–2799.

Mertens, D., Wolf, S., Schroeter, P., Schaffner, C., Dohner, H., Stilgenbauer, S., and Lichter, P. (2002). Down-regulation of candidate tumor suppressor genes within chromosome band 13q14.3 is independent of the DNA methylation pattern in B-cell chronic lymphocytic leukemia. Blood *99*, 4116–4121.

Meusser, B., Hirsch, C., Jarosch, E., and Sommer, T. (2005). ERAD: the long road to destruction. Nat. Cell Biol. *7*, 766–772.

Meyer, M., Gaudieri, S., Rhodes, D. A., and Trowsdale, J. (2003). Cluster of TRIM genes in the human MHC class I region sharing the B30.2 domain. Tissue Antigens *61*, 63–71.

Mitsiades, C. S., Mitsiades, N., Hideshima, T., Richardson, P. G., and Anderson, K. C. (2005). Proteasome inhibition as a therapeutic strategy for hematologic malignancies. Expert Rev. Anticancer Ther. *5*, 465–476.

Nakamura, M., Gotoh, T., Okuno, Y., Tatetsu, H., Sonoki, T., Uneda, S., Mori, M., Mitsuya, H., and Hata, H. (2006). Activation of the endoplasmic reticulum stress pathway is associated with survival of myeloma cells. Leuk. Lymphoma *47*, 531–539.

Nielsen, M. L., Savitski, M. M., and Zubarev, R. A. (2005). Improving protein identification using complementary fragmentation techniques in Fourier transform mass spectrometry. Mol. Cell Proteomics *4*, 835–845,

Nilsson, P. *et al.* (2005). Towards a human proteome atlas: high-throughput generation of mono-specific antibodies for tissue profiling. Proteomics *5*, 4327–4337.

Nuber, U., Schwarz, S. E., and Scheffner, M. (1998). The ubiquitin-protein ligase E6-associated protein (E6-AP) serves as its own substrate. Eur. J. Biochem. *254*, 643–649.

Obeng, E. A., Carlson, L. M., Gutman, D. M., Harrington, Jr., W. J., Lee, K. P., and Boise, L. H. (2006). Proteasome inhibitors induce a terminal unfolded protein response in multiple myeloma cells. Blood *107*, 4907–4916.

Ogawara, K. *et al.* (1998). Allelic loss of chromosome 13q14.3 in human oral cancer: correlation with lymph node metastasis. Int. J. Cancer *79*, 312–317.

Pagano, M., and Benmaamar, R. (2003). When protein destruction runs amok, malignancy is on the loose. Cancer Cell *4*, 251–256.

Panaretakis, T., Pokrovskaja, K., Shoshan, M. C., and Grander, D. (2003). Interferon-alpha-induced apoptosis in U266 cells is associated with activation of the proapoptotic Bcl-2 family members Bak and Bax. Oncogene *22*, 4543–4556.

Perkins, D. N., Pappin, D. J., Creasy, D. M., and Cottrell, J. S. (1999). Probability-based protein identification by searching sequence databases using mass spectrometry data. Electrophoresis *20*, 3551–3567.

Pickart, C. M. (2001). Mechanisms underlying ubiquitination. Annu. Rev. Biochem. *70*, 503–533.

Ravid, T., Kreft, S. G., and Hochstrasser, M. (2006). Membrane and soluble substrates of the Doa10 ubiquitin ligase are degraded by distinct pathways. EMBO J. *25*, 533–543.

Reimold, A. M. *et al.* (2001). Plasma cell differentiation requires the transcription factor XBP-1. Nature *412*, 300–307.

Reymond, A. *et al.* (2001). The tripartite motif family identifies cell compartments. EMBO J. *20*, 2140–2151.

Savitski, M. M., Nielsen, M. L., and Zubarev, R. A. (2005). New data base-independent, sequence tag-based scoring of peptide MS/MS data validates

Mowse scores, recovers below threshold data, singles out modified peptides, and assesses the quality of MS/MS techniques. Mol. Cell Proteomics *4*, 1180–1188.

Schmidt-Wolf, I. G. *et al.* (2006). Chromosomal aberrations in 130 patients with multiple myeloma studied by interphase FISH: diagnostic and prognostic relevance. Cancer Genet. Cytogenet. *167*, 20–25.

Shaughnessy, J. *et al.* (2000). High incidence of chromosome 13 deletion in multiple myeloma detected by multiprobe interphase FISH. Blood *96*, 1505–1511.

Shevchenko, A., Chernushevich, I., Wilm, M., and Mann, M. (2000). De novo peptide sequencing by nanoelectrospray tandem mass spectrometry using triple quadrupole and quadrupole/time-of-flight instruments. Methods Mol. Biol. *146*, 1–16.

Short, K. M., and Cox, T. C. (2006). Subclassification of the RBCC/TRIM superfamily reveals a novel motif necessary for microtubule binding. J. Biol. Chem. *281*, 8970–8980.

Song, B. L., Sever, N., and DeBose-Boyd, R. A. (2005). Gp78, a membrane-anchored ubiquitin ligase, associates with Insig-1 and couples sterol-regulated ubiquitination to degradation of HMG CoA reductase. Mol. Cell *19*, 829–840.

Stilgenbauer, S., Lichter, P., and Dohner, H. (2000). Genetic features of B-cell chronic lymphocytic leukemia. Rev. Clin. Exp. Hematol. *4*, 48–72.

Takahashi, R., and Imai, Y. (2003). Pael receptor, endoplasmic reticulum stress, and Parkinson's disease. J. Neurol. *250* (suppl 3), III25–29.

Torok, M., and Etkin, L. D. (2001). Two B or not two B? Overview of the rapidly expanding B-box family of proteins. Differentiation *67*, 63–71.

Trockenbacher, A., Suckow, V., Foerster, J., Winter, J., Krauss, S., Ropers, H. H., Schneider, R., and Schweiger, S. (2001). MID1, mutated in Opitz syndrome, encodes an ubiquitin ligase that targets phosphatase 2A for degradation. Nat. Genet. *29*, 287–294.

Urano, T., Saito, T., Tsukui, T., Fujita, M., Hosoi, T., Muramatsu, M., Ouchi, Y., and Inoue, S. (2002). Efp targets 14–3-3 sigma for proteolysis and promotes breast tumour growth. Nature *417*, 871–875.

Wada, M., Okamura, T., Okada, M., Teramura, M., Masuda, M., Motoji, T., and Mizoguchi, H. (2000). Delineation of the frequently deleted region on chromosome arm 13q in B-cell non-Hodgkin's lymphoma. Int. J. Hematol. *71*, 159–166.

Wang, Y., Li, Y., Qi, X., Yuan, W., Ai, J., Zhu, C., Cao, L., Yang, H., Liu, F., Wu, X., and Liu, M. (2004). TRIM45, a novel human RBCC/TRIM protein, inhibits transcriptional activities of ElK-1 and AP-1. Biochem. Biophys. Res. Commun. *323*, 9–16.

Vichi, A., Payne, D. M., Pacheco-Rodriguez, G., Moss, J., and Vaughan, M. (2005). E3 ubiquitin ligase activity of the trifunctional ARD1 (ADP-ribosylation factor domain protein 1). Proc. Natl. Acad. Sci. USA *102*, 1945–1950.

Wu, J., and Kaufman, R.J. (2006). From acute ER stress to physiological roles of the Unfolded Protein Response. Cell Death Differ. *13*, 374–384.

Yang, M., Omura, S., Bonifacino, J. S., and Weissman, A. M. (1998). Novel aspects of degradation of T cell receptor subunits from the endoplasmic reticulum (ER) in T cells: importance of oligosaccharide processing, ubiquitination, and proteasome-dependent removal from ER membranes. J. Exp. Med. *187*, 835–846.

Ye, Y. (2006). Diverse functions with a common regulator: Ubiquitin takes command of an AAA ATPase. J. Struct. Biol. *156*, 29–40.

Ye, Y., Meyer, H. H., and Rapoport, T. A. (2001). The AAA ATPase Cdc48/p97 and its partners transport proteins from the ER into the cytosol. Nature *414*, 652–656.

Zhong, X., Shen, Y., Ballar, P., Apostolou, A., Agami, R., and Fang, S. (2004). AAA ATPase p97/valosin-containing protein interacts with gp78, a ubiquitin ligase for endoplasmic reticulum-associated degradation. J. Biol. Chem. *279*, 45676–45684.

Zubarev, R. A., Horn, D. M., Fridriksson, E. K., Kelleher, N. L., Kruger, N. A., Lewis, M. A., Carpenter, B. K., and McLafferty, F. W. (2000). Electron capture dissociation for structural characterization of multiply charged protein cations. Anal. Chem. *72*, 563–573.